Pergamon

Geochimica et Cosmochimica Acta, Vol. 68, No. 17, pp. 3547–3555, 2004

0016-7037/04 $30.00 + .00

doi:10.1016/j.gca.2004.02.022

The flux of oxygen from the basal surface of gibbsite (α-$Al(OH)_3$) at equilibrium

JÖRGEN ROSENQVIST and WILLIAM H. CASEY*

Department of Land, Air, and Water Resources, and Department of Geology, University of California, Davis, Davis, CA 95616 USA

(*Received December* 5, 2003; *accepted in revised form February* 27, 2004)

Abstract—Experiments were conducted on gibbsite to determine whether oxygen-isotope exchange rates at hydroxyl bridges (μ_2-OH) on the basal sheet exhibit similar reactivity trends as in large aluminum polyoxocations, for which high-quality kinetic data exist. We followed the exchange of ^{18}O from the mineral surface to solution by using a high-surface-area solid that had been enriched to tens of *percent* in ^{18}O. To establish this high enrichment, we initially react the solid hydrothermally with highly enriched $H_2^{18}O$ in order to tag all oxygens near the mineral surface, and then back exchange the most reactive oxygens with isotopically normal water. This enrichment procedure isolates ^{18}O into the least-reactive sites, which are presumably μ_2-OH on the basal surface. By analogy with aqueous aluminum complexes, including large multimers, the η-OH_2 sites exchange within fractions of a second and should be isotopically normal using this procedure.

When suspended in isotopically normal electrolyte solutions, we find that the rates of release of ^{18}O from the mineral fall close to the rates of dissolution. The lack of steady isotopic exchange of μ_2-OH on gibbsite surfaces contrasts with the aluminum polyoxocations, where the μ_2-OH exchange many hundreds of times with bulk water molecules before the molecule dissociates. Additional experiments were conducted in solutions at near-neutral pH to determine the flux of oxygens at conditions near thermodynamic equilibrium. As in more acidic solutions, rates are close to values expected from dissolution of the mineral and there is no evidence for steady exchange of hydroxyl bridges with water molecules in the bulk solution. *Copyright © 2004 Elsevier Ltd*

1. INTRODUCTION

Advances in X-ray spectroscopy led geochemists to recognize that metal adsorbates often polymerize into secondary minerals by combining with the aluminum that is released by slow dissolution of clays (e.g., Charlet and Manceau, 1992; O'Day et al., 1994; d'Espinose de la Caillerie et al., 1995; Thompson et al., 1999; Scheidegger et al., 1998). To establish a quantitative model for these reactions, geochemists need information about the rates of polymerization of mineral surfaces, and particularly near thermodynamic equilibrium. Although high-quality kinetic studies exist for 1–2 nm-sized aluminum polyoxocations [$\mathbf{Al}_{13}$ = $AlO_4Al_{12}(OH)_{24}(H_2O)_{12}^{7+}$; $\mathbf{Al}_{30}$ = $Al_2O_8Al_{28}(OH)_{56}(H_2O)_{26}^{18+}$; see Table 1], these experiments yield puzzling results because the hydroxyl bridges in these molecules exchange oxygen isotopes with solution much more rapidly than the molecules dissociate. Hydroxyl bridges between two Al(III) atoms (μ_2-OH) exchange over time scales that vary from seconds to months at 298 K. Conversely, the bound waters (η-OH_2) isotopically exchange with bulk solution within milliseconds at 298 K and fall within the same range as aluminum monomer complexes (Table 1). The structural formalism (μ_2-OH, η-OH_2) indicates oxygen coordination chemistry but not charge and the protonation states can change with pH.

These results plea for direct studies of the surfaces of minerals like gibbsite, that also expose η-OH_2 and μ_2-OH sites to solution (Fig. 1). This mineral has a particularly simple surface chemistry, although the oxygens can change protonation states and one expects that the reactivities of μ_2-OH at the basal plane and at crystallite edges will differ considerably. It is yet impossible to determine rates of oxygen exchanges at the gibbsite surface using ^{17}O-NMR spectroscopy (see Walter and Oldfield, 1989), as was done for the $\mathbf{Al}_{13}$ and $\mathbf{Al}_{30}$ polyoxocations. Therefore, we here report results using classical ^{18}O-exchange experiments and try to isolate the least-reactive oxygens that lie in μ_2-OH sites on the basal plane.

There are two potential contributions to the oxygen flux from μ_2-OH sites on the basal plane of gibbsite: (i) steady exchange of oxygens with bulk-solution water molecules via a proton-enhanced pathway that does not depolymerize the surface; and (ii) dissolution of the surface by retreat of monomolecular steps, that releases the oxygens as inner-sphere water molecules bound to aqueous aluminum complexes. Reaction via these two pathways, of course, could potentially proceed simultaneously. For the $\mathbf{Al}_{13}$ and $\mathbf{Al}_{30}$ molecules, exchange via the first pathway could be via proton transfer that converts a μ_2-OH bridge to a weak μ_2-OH_2 bridge, followed by exchange of this bridge with a bulk water molecule and then deprotonation to reform the μ_2-OH bridge (see Casey et al., 2000, 2001; Casey and Swaddle, 2003). Exchange via the second pathway entails complete dissociation of the $\mathbf{Al}_{13}$ and $\mathbf{Al}_{30}$ molecules into monomeric complexes that exchange their oxygens with bulk solution within seconds. This comparison gives rise to some clear questions:

Question 1) Do the μ_2-OH at the gibbsite surface exchange oxygens with bulk solution more rapidly than the mineral dissolves?

Question 2) Does deprotonation of the gibbsite surface, which is manifested as changes in surface-charge density (e.g., Hiemstra et al., 1999), affect rates of exchange of oxygens in μ_2-OH?

The rates of exchange at η-OH_2 sites are expected to increase dramatically with pH, by analogy with ligand-exchange

* Author to whom correspondence should be addressed (whcasey@ucdavis.edu).

Table 1. Characteristic times for exchange of bound water molecules (η-OH_2) and hydroxyl bridges between two metals (μ_2-OH) from the inner-coordination sphere of Al(III) with the bulk solution at 277 K, 298 K and 323 K. The characteristic times are estimated from the pseudo-first-order rate coefficients (k_{ex}) according to: $\tau = 1/k_{ex}$. Sources are listed in Casey et al (2001).

Species	τ_{277} (s)	τ_{298} (s)	τ_{323} (s)
	Bound waters (η-OH_2) *monomeric complexes*		
$Al(H_2O)_6^{3+}$	10.4 ($\pm$0.3)	7.8 ($\pm$0.2) $\cdot 10^{-1}$	5.4 ($\pm$0.2) $\cdot 10^{-2}$
$AlOH^{2+}$	9.7 ($\pm$3.2) $\cdot 10^{-5}$	3.2 ($\pm$1.0) $\cdot 10^{-5}$	1.0 ($\pm$0.4) $\cdot 10^{-5}$
AlF^{2+}	4.7 ($\pm$0.8) $\cdot 10^{-2}$	4.2 ($\pm$0.6) $\cdot 10^{-3}$	3.5 ($\pm$0.6) $\cdot 10^{-4}$
AlF_2^{+}	4.4 ($\pm$0.3) $\cdot 10^{-4}$	6.1 ($\pm$0.4) $\cdot 10^{-5}$	8.0 ($\pm$0.5) $\cdot 10^{-6}$
$Al(ox)^{+}$	7.6 ($\pm$1.1) $\cdot 10^{-2}$	9.2 ($\pm$1.3) $\cdot 10^{-3}$	1.1 ($\pm$0.2) $\cdot 10^{-3}$
	multimeric complexes		
Al_{13}	4.6 ($\pm$0.5) $\cdot 10^{-3}$	9.1 ($\pm$0.9) $\cdot 10^{-4}$	1.7 ($\pm$0.2) $\cdot 10^{-4}$
$GaAl_{12}$	3.0 ($\pm$0.7) $\cdot 10^{-2}$	4.4 ($\pm$1.0) $\cdot 10^{-3}$	6.2 ($\pm$1.3) $\cdot 10^{-4}$
$GeAl_{12}$	2.9 ($\pm$0.9) $\cdot 10^{-2}$	5.3 ($\pm$1.5) $\cdot 10^{-3}$	9.2 ($\pm$2.7) $\cdot 10^{-4}$
	Hydroxyl bridges (μ_2-OH)		
Al_{13}			
μ_2-OH^{fast}	3.0 ($\pm$1.0) $\cdot 10^{4}$	6.3 ($\pm$2.0) $\cdot 10^{1}$	1.1 ($\pm$0.4) $\cdot 10^{-1}$
μ_2-OH^{slow}	1.5 ($\pm$0.1) $\cdot 10^{6}$	6.3 ($\pm$0.4) $\cdot 10^{4}$	2.4 ($\pm$0.2) $\cdot 10^{3}$
$GaAl_{12}$			
μ_2-OH^{fast}	1.1 ($\pm$0.1) $\cdot 10^{6}$	5.6 ($\pm$0.3) $\cdot 10^{4}$	2.6 ($\pm$0.1) $\cdot 10^{3}$
μ_2-OH^{slow}	1.1 ($\pm$0.1) $\cdot 10^{8}$	2.4 ($\pm$0.2) $\cdot 10^{6}$	4.9 ($\pm$0.3) $\cdot 10^{4}$
$GeAl_{12}$			
μ_2-OH^{fast}	minutes or less	minutes or less	minutes or less
μ_2-OH^{slow}	1.9 ($\pm$0.1) $\cdot 10^{4}$	1.5 ($\pm$0.1) $\cdot 10^{3}$	1.2 ($\pm$0.1) $\cdot 10^{2}$

abbreviations: $Al_{13} = AlO_4Al_{12}(OH)_{24}(H_2O)_{12}^{7+}$(aq); $GaAl_{12} = GaO_4Al_{12}(OH)_{24}(H_2O)_{12}^{7+}$(aq); and $GeAl_{12} = GeO_4Al_{12}(OH)_{24}(H_2O)_{12}^{8+}$(aq); ox = oxalate.

rates in aqueous complexes. For example, the rates of exchange of a bound water in the $AlOH(OH_2)_5^{2+}$ complex is $\sim 10^4$ times faster than the $Al(OH_2)_6^{3+}$ complex (Nordin et al., 1998). However, the dependence of exchange rates on μ_2-OH sites on pH is largely unknown. For the $\mathbf{Al}_{13}$ and $\mathbf{Al}_{30}$ molecules the accessible pH range is too narrow to unambiguously answer questions about the effect of deprotonation on the exchange rates on μ_2-OH sites. The gibbsite surfaces are positively charged throughout the pH range studied here (3–7) but there is an appreciable change in the ratio between protonated and deprotonated surface groups. Further details about the protonation/deprotonation of gibbsite surfaces can be found in Rosenqvist et al. (2002).

Any aluminum complexes that are released to the aqueous solution by dissolution of gibbsite would exchange oxygens isotopes with bulk solution in fractions of a second. Therefore, if the surface of ^{18}O-rich gibbsite were recrystallizing by the advance and retreat of elementary steps on the basal plane (see Peskleway et al., 2003), one would observe a flux of ^{18}O to the aqueous solution even though there were no measurable change in dissolved aluminum concentration or pH. This steady flux can be expressed using the rate laws that ignore the molecular details, yet which are familiar to those geochemists who study mineral dissolution. For any elementary reaction written in this form: $\sum_{i=1}^{n} \nu_i \cdot R_i = \sum_{j=1}^{m} \lambda_j \cdot P_j$, the net rate of reaction can be separated into contributions from the forward and reverse reactions:

$$r_{net} = \vec{r} - \overleftarrow{r} \tag{1}$$

$$r_{net} = \vec{k} \prod_{i=1}^{n} [R_i]^{\nu_i} - \overleftarrow{k} \prod_{j=1}^{m} [P_j]^{\lambda_j} \tag{2}$$

where: $[R_i]$ and $[P_j]$ represent the molalities of reactant *'i'* and product *'j'*, respectively, ν_i and λ_j are the stoichiometric coefficients, which also correspond to rate orders since these are elementary reactions, and Equations 2 and 3 are rate coefficients for the forward and reverse reaction steps. At equilibrium, Eqn. 3 is satisfied:

$$\vec{k} \prod_{i=1}^{n} [R_i]^{\nu_i} = \overleftarrow{k} \prod_{j=1}^{m} [P_j]^{\lambda_j} \neq 0 \tag{3}$$

as the rates in the forward and reverse directions are equal, but not necessarily zero.

Although Eqns. (1)–(3) correspond to an elementary reaction, the result can be made general through choice of an appropriate average stoichiometric number (Temkin, 1971; Boudart, 1976) that scales the overall reaction Gibbs energy, which is easily calculated, to equal the Gibbs energy of the rate-controlling step. In no geochemical reaction is the Gibbs energy of the rate-controlling step confidently known, so these stoichiometric numbers are *de facto* adjustable parameters that are modified to make the rate law fit the experimental data as experiments approach equilibrium. Adjustments can easily be made to the equations to account for heterogeneous reactions. The important point is that a conventional mineral-dissolution experiment cannot detect the directional flux at equilibrium because only the *net* change of a solute concentration, such as dissolved Al(III) or protons, is detected.

The important point is that there should be a measurable flux of oxygens from a mineral surface near equilibrium due to advance and retreat of elementary, or to rapid isotopic exchange at individual oxygen sites via a proton-enhanced pathway. This flux could be measured by making the surface oxygens isotopically unique. Previously this approach was difficult because geochemists had no knowledge of the relative rates of different oxygen sites. From experiments on the 1–2

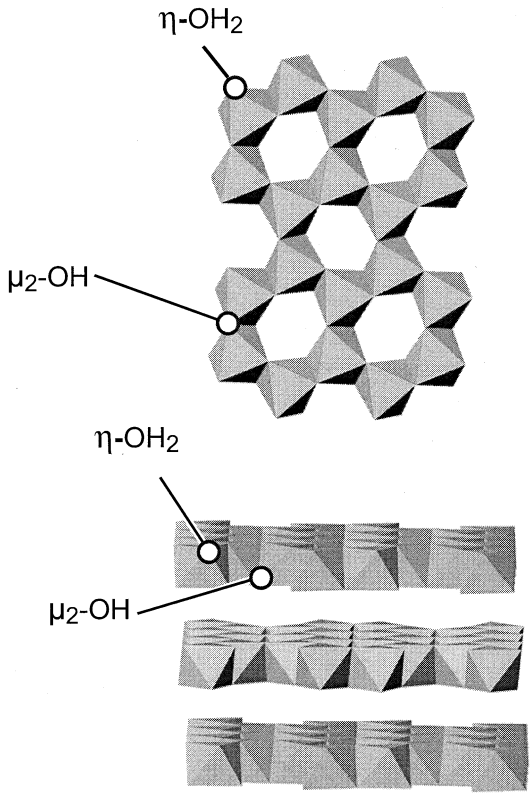

Fig. 1. Polyhedral representations of gibbsite. The {001} face is shown at the top and the {010}face is shown on the bottom, with both orientations in the plane of the paper. Oxygens as bound water molecules (η-OH_2) and as hydroxyl bridges between two aluminums (μ_2-OH bridges) are identified.

nm sized aluminum-hydroxide clusters, we now know that the η-OH_2 exchange many orders of magnitude more rapidly than the μ_2-OH [Table 1] and this difference can be exploited to create a surface that is isotopically enriched in μ_2-^{18}OH and η-$^{16}OH_2$.

2. EXPERIMENTAL METHODS

2.1. Rate Measurements

The use of $^{18}O/^{16}O$ ratios to follow ligand-exchange reactions at mineral surfaces is rarely undertaken at low temperatures (see Cole and Chakraborty, 2001 for review). The problem is a matter of sensitivity. Even if the surface oxygens are enriched to tens of per mil in $\delta^{18}O$, one usually cannot observe a measurable change in $\delta^{18}O$ values of the aqueous solution as these oxygens exchange with bulk waters. The following calculation illustrates the problem. Most mineral powders have specific surface areas in the range 0.01 to 1 m^2/g. Assuming an area of 1 m^2/g and an oxygen-site density of 10 sites/nm^2, the total number of surface oxygens is: 1 m^2/g * 10^{18} nm^2/m^2 *10 nm^{-2}/6.022 $\cdot$ 10^{23} mol^{-1} = 1.66 $\cdot$ 10^{-5} mol/g. In Standard-Mean Ocean Water (SMOW) the percentage of ^{18}O is 0.20052%. If this mineral had a 10 ‰ enrichment in $\delta^{18}O$, the corresponding proportion of ^{18}O would be 0.20253%. The number of surface sites with ^{18}O can therefore be calculated as: 1.66 $\cdot$ 10^{-5} mol/g * 0.20253% = 3.36 $\cdot$ 10^{-8} mol/g. A flux of ^{18}O from the mineral could be measured easily if the solution exhibited a range of $\delta^{18}O$ of ~1 ‰, but the number of ^{18}O atoms needed to achieve this range is: 1 ‰ * 0.20052% * 55.5 mol/L = 1.11 $\cdot$ 10^{-4} mol/L. The solid concentration required to achieve this signal is: 1.11 $\cdot$ 10^{-4} mol/L/3.36 $\cdot$ 10^{-8} mol/g = 3309 g/L, which is impossibly high.

The method can, however, be modified to become more sensitive. Use of nanometer-size particles can increase the surface area considerably. Also, water that is enriched in the range of 10–95% ^{18}O is now commercially available and a mineral treated with such a solution would have a concentration of ^{18}O at the mineral surface that is several *percent* (not per mil) ^{18}O. As we show, these adaptations increase the sensitivity of the method and make it possible to measure fluxes from gibbsite surfaces even at low temperatures. Hypothetically, sensitivity could also be improved by studying ^{17}O instead of ^{18}O, as the natural abundance of ^{17}O is about five times lower (0.037% versus 0.20052%). However, eliminating the contribution to the mass 45/44 signal from the ^{13}C content of the CO_2 gas can be complicated. We found that small fluctuations in the ^{13}C content significantly affected the $\delta^{17}O$ signal so we chose to follow the flux of ^{18}O from the gibbsite surface, not ^{17}O.

2.2. Solid Material

Gibbsite of uniform size was prepared using a method similar to Gastuche and Herbillon (1962). Briefly, a 1 mol/L $AlCl_3$ solution was titrated with 4 mol/L NaOH until pH ~4.6, at which amorphous aluminum hydroxide precipitated. The suspension was heated for 2 h at 313 K, transferred into Spectra/Por® cellulose-ester dialysis membranes and dialyzed against 18 MΩ cm^{-1} water at 323 K for 4 weeks. The dialysis water was refreshed daily during the first two weeks and every second day thereafter. The resulting suspension had a solid content of ~12 g/L. The X-ray diffraction pattern showed well-resolved peaks that are characteristic for gibbsite and no signs of other crystalline phases were detected.

Scanning-electron microscopy (SEM) images of the gibbsite sample [Figure 2] showed it to consist of thin, pseudohexagonal platelets. To enrich the surface of this gibbsite in ^{18}O we reacted it at 388 K for 24 h (see below). This hydrothermal treatment caused a slight change to the initial dimensions of the platelets, increasing the thickness and decreasing the diameter. This thickening occurred by deposition of material in ^{18}O enriched water, so the basal planes must be enriched in ^{18}O. The isotope composition of the edge planes is more difficult to gauge, since the decreased diameter indicates that the edges dissolve during the hydrothermal treatment. The particle dimensions were determined from the electron micrographs using standard image-analysis software and, after the hydrothermal treatment, the particles had a diameter of 209(±43) nm and a thickness of 49(±27) nm (n = 1400). Using the particle dimensions and a density of 2.414 g/cm^3 for gibbsite (Saalfeld and Wedde, 1974), a total surface area of 25 m^2/g, distributed as 7.9 m^2/g edge area and 17 m^2/g basal plane area, was calculated. The BET area was measured using N_2 adsorption (5 points) and found to be 19.6(±0.1) m^2/g. To conform to earlier reports on fluxes from mineral surfaces (e.g., Nagy, 1995), all calculations were performed using the BET surface area.

2.3. Experimental Procedure

The flux of ^{18}O from gibbsite surfaces was followed in a series of experiments at 323 K at different pH values [Table 2] in 0.010 mol/L NaCl ionic medium. The only exceptions were experiments #1 and #2, both at pH 2.5, which were performed in 0.100 mol/L NaCl medium to avoid excessively high liquid-junction potentials. For the experiments at low pH (2.5 ≤ pH ≤ 4.5) a pH-stat apparatus was employed along with a Metrohm combination electrode, filled with the ionic medium. The electrode was calibrated in separate titrations before, and after, the oxygen-exchange experiment and 0.001 mol/L or 0.010 mol/L HCl solutions were added to keep pH constant. In the pH = 6 and pH = 7 experiments, buffer solutions were used to control pH. For experiments at pH = 6, a 0.010 mol/L buffer solution was prepared from solid MES (4-Morpholinoethanesulfonic acid) and 1 N NaOH. For the experiment at pH = 7, a 0.010 mol/L solution of PIPES (1,4-piperazinebis(ethanesulfonic acid)) and NaOH was used. In experiment # 15 (Table 2), the pH was allowed to drift freely and the solution reached pH = 7.1 in a few days. In the pH-stat experiments, the fluxes of protons, soluble aluminum and ^{18}O were measured simultaneously, whereas for the near-neutral pH experiments only the ^{18}O flux was measured. At near-neutral pH and 323 K, the solubility of gibbsite is on the order of ~10^{-7} M (Wesolowski and Palmer, 1994), which is well below our detection limit.

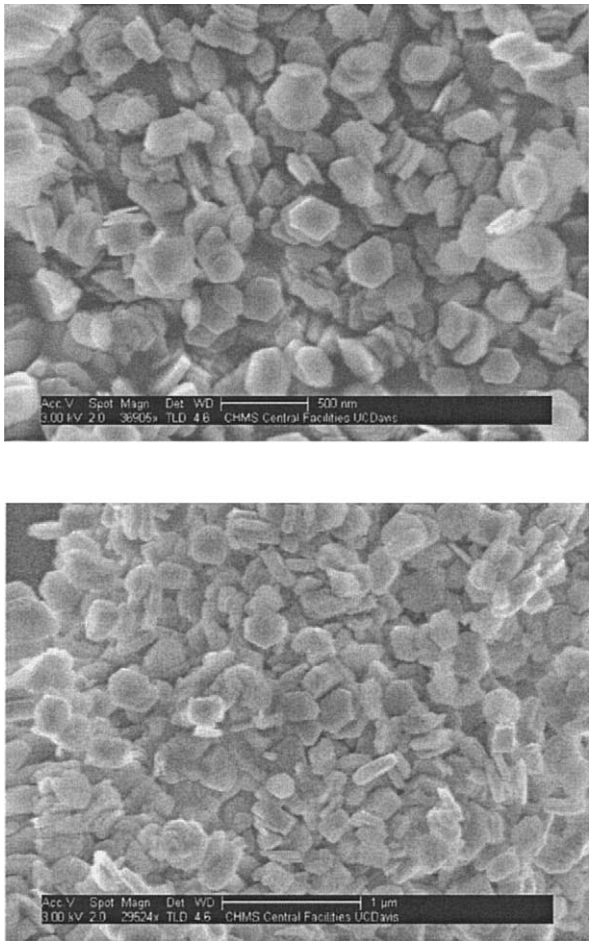

Fig. 2. SEM images of untreated (top) and hydrothermally reacted gibbsite (bottom).

Each experiment was started by equilibrating a gibbsite suspension (typically 30 mL) at the desired pH value [Table 2] in ionic medium at 323 ± 0.5 K. These equilibrations were conducted for either one week or overnight, depending upon the goals of the particular experiment. Gibbsite particles were then separated by centrifugation at 24 000 g and resuspended in 1 mL $H_2{}^{18}O$ enriched water (6%, 11.5% or 84% $H_2{}^{18}O$, Isotec Labs). The suspension was transferred to a 10 mL polycarbonate centrifuge tube and placed in a hydrothermal reactor, where it was reacted at 388 K for 24 h. The suspension was then again centrifuged at 24 000 g at 273 K and the $H_2{}^{18}O$ was collected. Diluted samples from the $H_2{}^{18}O$ were analyzed using mass spectrometry to determine the ^{18}O concentration. The particles were washed three times with isotopically normal water (precooled to 277 K) to remove any entrained bulk $H_2{}^{18}O$. In the last washing step, the suspension was sonicated for 2 min before centrifugation.

The rinsing step is important because it is intended to exchange oxygens in the η-$^{18}OH_2$ sites at particle edges with $H_2{}^{16}O$ in bulk water. Studies of aluminum monomers and 1–2 nm sized polyoxocations ($\mathbf{Al}_{13}$; $\mathbf{Al}_{30}$) indicate that the η-OH_2 probably exchange oxygen isotopes within seconds at 277 K [Table 1]. In contrast, the hydroxyl bridges probably retain the ^{18}O at the surface oxygens during this rinsing. The rates of exchange of μ_2-OH sites in the $\mathbf{Al}_{13}$ and $\mathbf{Al}_{30}$ polyoxocations, which we employ as a guide to possible results on gibbsite, are too slow to allow isotopic equilibration of more than a percent of the hydroxyl bridges during the rinsing step. We also found in preliminary experiments at low temperatures that the flux of ^{18}O from the gibbsite surfaces was much slower than predicted from the data for multimeric aluminum complexes. Therefore, all gibbsite dissolution experiments were performed at 323 K, although rinsing was performed at 277 K.

The last part of the experiment was begun when the washed particles were resuspended in 30 mL of solution at 323 K. Depending upon the goals of the particular experiment, these solutions were either fresh ionic medium or ionic medium that had been saved from the equilibration step and stored at 323 K. After initiating an experiment, two-milliliter samples of the gibbsite suspension were collected periodically over the next days or weeks. Solids were removed from these samples by centrifugation (7500 g, 273 K) in Millipore Ultrafree-CL centrifugal filter devices (filter pore size 0.1 μm). The ^{18}O concentration in the fluid was determined by mass spectrometry. For the low pH samples, a small part of the solution was diluted, acidified and analyzed for soluble aluminum using an ICP-MS instrument. The centrifugal filters were dried and weighed to determine the solid concentration.

2.4. ^{18}O Measurements

The sample water was equilibrated with CO_2 at constant temperature for ten hours. The CO_2 was then extracted from the reaction vessel, treated to remove water and analyzed on a Finnigan MAT 251 Isotope-Ratio Mass Spectrometer versus a reference CO_2. Because we want to estimate ^{18}O fluxes, it is most convenient to express the concentrations of ^{18}O in molar units [Appendix 1]. The precision of measurement is better than ± 0.01 mM (1σ) as determined by repeated analysis of samples and standards.

3. RESULTS

The pH of the suspensions typically decreased slightly during the hydrothermal treatment and increased again during a dissolution experiment if not controlled. The pH drift, when uncontrolled, was usually less than a pH unit. We nevertheless eliminated the pH drift by employing a pH-stat method in acidic solutions and through use of buffer solutions in near-neutral-pH experiments. The pH-stat experiments at lower pH were intended to relate the ^{18}O fluxes to dissolution rates of the mineral.

In experiments #11–15, the ^{18}O tagged particles were suspended into the same solution in which they had previously reacted. These solutions were presumably saturated with respect to gibbsite, so that the ^{18}O-flux would correspond to conditions close to equilibrium, as described by Eqn. (1)-(3). The observed fluxes of ^{18}O, protons and soluble aluminum are listed in Table 3, and the results from different techniques for one experiment are shown in Figure 3. The rapid release of ^{18}O in the beginning of the experiment may be due to minor amounts of entrained $H_2^{18}O$ that was not fully removed by the washing step, or to oxygen sites at the crystallite edges that react much more rapidly than those on the basal plane, or to particularly reactive sites that are eliminated rapidly by dissolution. Nevertheless, excluding these first few points in each experiment gives linear relationships between ^{18}O concentra-

Table 2. Experimental conditions.

Experiment #	Equilibration pH	Reaction pH	pH control
1, 2	4.0	2.5	pH stat
3–6	4.0	3.0	pH stat
7, 8	4.0	3.5	pH stat
9, 10	4.0	4.0	pH stat
11, 12	4.5	4.5	pH stat
13	6.0	6.0	MES buffer
14	7.0	7.0	PIPES buffer
15	7.5	6.7-7.1	None

Table 3. Observed fluxes (in mol m^{-2} s^{-1}) of gibbsite from the different experiments, according to different analytical techniques. All values are expressed per square meter of total BET area. Included are also numbers from experiments performed in isotopically normal water. Uncertainties are assigned from the standard error of the regression.

Exp. #	pH	Protons	Aluminum	^{18}O
1	2.5	$5.7 \cdot 10^{-11}$	$4.1 (\pm 0.1) \cdot 10^{-11}$	$3.7 (\pm 0.4) \cdot 10^{-11}$
2	2.5	—	$3.5 (\pm 0.1) \cdot 10^{-11}$	—
3	3.0	$4.1 \cdot 10^{-11}$	$3.0 (\pm 0.1) \cdot 10^{-11}$	$2.0 (\pm 0.9) \cdot 10^{-11}$
4	3.0	$5.4 \cdot 10^{-11}$	$3.3 (\pm 0.1) \cdot 10^{-11}$	$3.1 (\pm 0.7) \cdot 10^{-11}$
5	3.0	$3.2 \cdot 10^{-11}$	$3.0 (\pm 0.2) \cdot 10^{-11}$	—
6	3.0	$3.8 \cdot 10^{-11}$	$3.5 (\pm 0.1) \cdot 10^{-11}$	—
7	3.5	$1.2 \cdot 10^{-11}$	$7.7 (\pm 0.3) \cdot 10^{-12}$	$2.0 (\pm 0.6) \cdot 10^{-11}$
8	3.5	$9.5 \cdot 10^{-12}$	$7.6 (\pm 1.1) \cdot 10^{-12}$	—
9	4.0	$2.0 \cdot 10^{-12}$	$1.3 (\pm 0.3) \cdot 10^{-12}$	$2.8 (\pm 0.2) \cdot 10^{-11}$
10	4.0	$1.7 \cdot 10^{-12}$	$8.0 (\pm 1.1) \cdot 10^{-13}$	—
11	4.5	—	—	$2.1 (\pm 0.1) \cdot 10^{-11}$
12	4.5	$3.4 \cdot 10^{-12}$	—	$1.3 (\pm 0.1) \cdot 10^{-11}$
13	6.0	—	—	$3.8 (\pm 0.3) \cdot 10^{-12}$
14	7.0	—	—	$4.5 (\pm 0.6) \cdot 10^{-12}$
15	6.7-7.1	—	—	$2.3 (\pm 0.2) \cdot 10^{-12}$

tion and time, allowing calculation of the flux of ^{18}O, which is close to the dissolution rates of the solid [Table 3 and Figures 3–5]. The difference in fluxes estimated by proton, ^{18}O and aluminum concentrations as a function of time are small relative to other uncertainties in estimates of the absolute rates. The uncertainties given for aluminum and ^{18}O in Table 3 are standard deviations from the linear regression. Because there are so many points in the pH measurements, these standard deviations are deceptively small; for the proton-flux data, the uncertainty is probably on the order of one percent. Repeated experiments yield rates that are reproducible to within about twenty percent [Table 3]. As we discuss below, however, the systematic uncertainties in the rate estimates are probably much higher than the experimental precision. For example, one large uncertainty in our ^{18}O flux estimate is the estimated fraction of ^{18}O at the surface of the mineral. We used as our estimate the

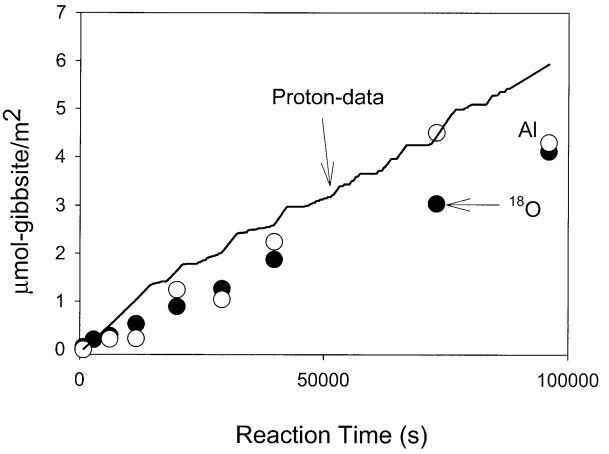

Fig. 3. Results from gibbsite dissolution experiment at pH 2.5 (exp. #1). The fluxes are expressed as flux of gibbsite per square meter of total BET area, i.e., the fluxes of protons and oxygens have been divided by a factor of three.

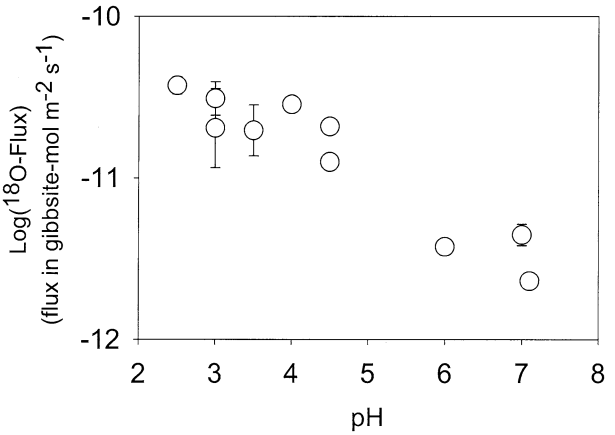

Fig. 4. The logarithm in base ten of the fluxes of ^{18}O from gibbsite at different pH conditions.

measured ^{18}O concentration of the solution used in the hydrothermal enrichment step, but *after* the enrichment reaction was complete. Isotopic exchange between this solution and the gibbsite surface was sufficient to change the ^{18}O concentration of the solution by many percent.

The efficiency of the hydrothermal treatment was evaluated in an experiment where the treated gibbsite particles were totally digested in strong acid and the resulting ^{18}O concentration of the solution was measured. The results indicated that the oxygens in the first seven to eight layers of an average-sized particle had been isotopically exchanged, if we assume an even distribution of ^{18}O over the surface. In contrast, the amount of ^{18}O released to the solution in a dissolution experiment was equivalent to less than a single monolayer of gibbsite. We cannot, of course, prove that the ^{18}O flux is only from the surface μ_2-OH at the basal plane, although the results are not particularly sensitive to exchange of oxygens from the crystallite edges since these contributions are relatively small. Crystallographically, a gibbsite particle exposes 13.7 μ_2-OH sites per nm^2 of basal area and 8.8 μ_2-OH and 8.8 η-OH_2 sites per nm^2 of edge (e.g., Rosenqvist et al., 2002). For the experiment at pH = 2.5 [Figure 3], for example, the total contribution from η-OH_2 (present at the surface only) would amount only to 0.12 μmol/m^2, which is much smaller than the total flux of ^{18}O to solution. As stated above, the η-OH_2 sites should have been isotopically equilibrated in our rinsing steps. The μ_2-OH sites at the particle edges might contribute more to the total ^{18}O flux. However, for a gibbsite particle that is 200 nm in breadth and 50 nm in thickness, the μ_2-OH sites on the edges only amount to ~23% of the total μ_2-OH sites.

4. DISCUSSION

These experiments provide clear answers to **Question 1** and **Question 2,** posed above. First, there is no rapid and steady exchange of oxygens between μ_2-OH sites on the basal plane of gibbsite and bulk water molecules. In all cases, the ^{18}O fluxes were close to those expected from dissolution of the solid [Figures 4, 5]. Secondly, the rates *decrease* with increased pH, as one expects from dissolution, but opposite to that

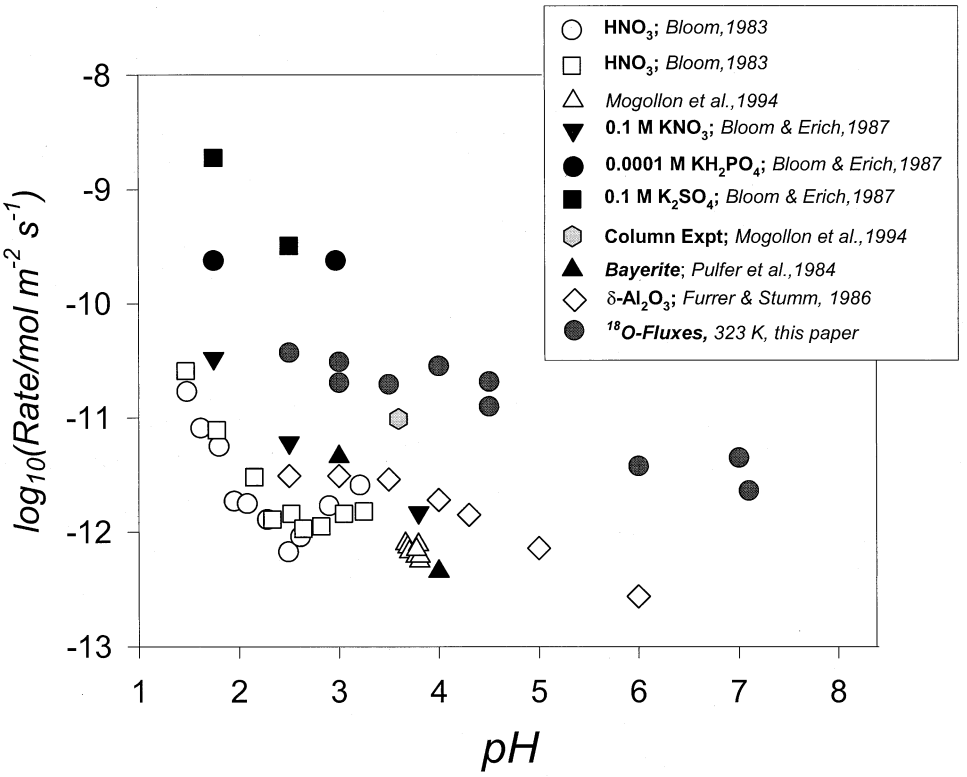

Fig. 5. The ^{18}O fluxes from gibbsite measured at 323 K compared with rates of dissolution determined by monitoring aluminum and proton fluxes at 298 K (from Nagy, 1995). The difference in temperature undoubtedly accounts for the fact that the fluxes of ^{18}O are slightly higher than dissolution rates at 298 K. The important point is that the rates fall within the same general range and exhibit a similar pH dependence.

predicted from the kinetics of ligand-exchange reactions where deprotonation commonly accelerates rates.

Our interpretation is that oxygen fluxes at the mineral surface correspond to the steady advance and retreat of steps on the basal plane, which can occur even when there is no net dissolution rate. These movements yield the flux of ^{18}O that is measurable at near-neutral pH, in solutions that are presumably near thermodynamic equilibrium with the suspended solid. We recognize that these rates probably correspond to high estimates of the true steady-state flux because several researchers have shown that dissolution rates determined in short-term experiments, such as these, are commonly much more rapid than in longer-term experiments (e.g., Strandh 1999). The important point, however, is that there is no steady exchange of μ_2-^{18}OH apart from dissolution of the mineral surface, during which the μ_2-^{18}OH sites are hydrolyzed to form η-OH_2 (and η-OH) sites.

These measurements lead us to speculate about the reactive lifetimes of different surface oxygens on gibbsite. In these experiments, the lifetime of oxygens in μ_2-OH on the basal planes of gibbsite is ~50 d or greater at 323 K, which is estimated by calculating the time necessary to remove a monolayer of mineral from the basal sheet using the data compiled in Table 3 for the pH range 6–7. For comparison, μ_2-OH in the $\mathbf{Al}_{13}$ molecule exchange within 0.1 s and 40 min at 323 K [Table 1]. By analogy with aqueous aluminum complexes [Table 1], η-OH_2 bound to the edges of gibbsite probably exchange with the bulk solution in timescales of milliseconds or less.

The rates of exchange of the μ_2-OH sites at edges of the crystals are difficult to estimate with confidence. It is possible that the edge μ_2-OH can form hydrogen bonds to adjacent η-OH_2 groups, since the distance between a μ_2-OH and a η-OH_2 site on the gibbsite edges is (probably) ~2.7–2.8 Å (as calculated from the bulk structure) and the different groups exist in a 1:1 ratio. The O-O distance in structures with considerable hydrogen-bonding, such as potassium-dihydrogen phosphate, is commonly near 2.50 Å (Nelmes et al., 1982).

The possibility of hydrogen bonding to a bound water molecule, forming a $H_3O_2^-$ moiety, introduces an important pathway for isotopic exchange that does not exist for μ_2-OH sites on the basal planes. To exchange oxygen isotopes, the $H_3O_2^-$ moiety need only exchange the positions of the η-OH_2 and μ_2-OH within the $H_3O_2^-$ moiety. Such a mechanism for oxygen-isotope exchange is illustrated in Figure 6. The first step is rapid exchange of a η-OH_2 with a bulk water molecule, followed by hydrogen bonding between the η-OH_2 to the adjacent μ_2-OH to form the $H_3O_2^-$ structure. Exchange of positions leads to isotopic enrichment in the edge μ_2-OH. We can assign a characteristic time of hours for these exchanges at 323 K by analogy with the rates observed for polyoxocations, which also have μ_2-OH adjacent to η-OH_2. We recognize that these estimates are highly uncertain, yet can be improved with further experiments using this ^{18}O-enrichment method.

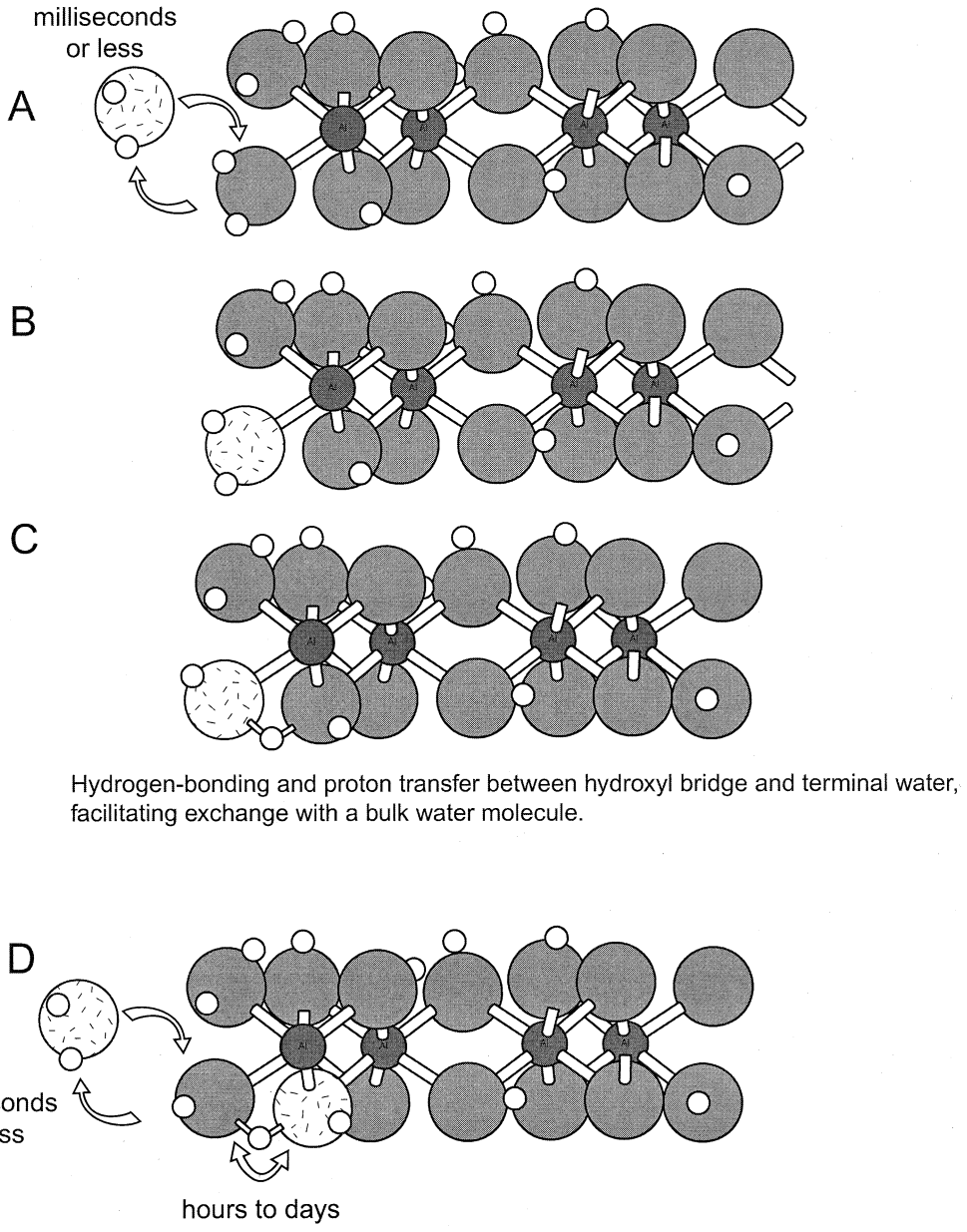

Fig. 6. A schematic diagram illustrating a possible isotope-exchange pathway at μ_2-OH on the edges of gibbsite. These μ_2-OH bridges at crystallite edges may react much more rapidly than those μ_2-OH situated in six-membered rings on the basal plane because the hydrogen-bonding to adjacent nonbridging η-OH_2 leads to exchange of positions and, hence, oxygen-isotope exchange.

5. CONCLUSIONS

There are key observations reported here that help organize reactivity trends for other minerals:

1) The oxygen fluxes from gibbsite basal planes are controlled by the retreat and advance of surface steps that convert μ_2-OH bridges to η-OH_2, and back (Fig. 7). This steady recrystallization of the gibbsite surface yields a measurable flux of oxygen isotopes to the aqueous solution, even at equilibrium, because η-OH_2 exchange oxygen isotopes in fractions of a second whereas oxygens in the basal μ_2-OH bridges are inert. Similar rates are expected for the basal planes of other dioctahedral clays that expose a gibbsite-like surface to the aqueous solution. The dissolution rates for these minerals are often known (e.g., Nagy, 1995), yielding testable hypotheses about the oxygen fluxes.
2) These experiments are consistent with conclusions derived from isotope-exchange experiments on minerals at higher temperature (see Cole and Chakraborty, 2001). Previous workers commonly found that near-surface isotope exchange involves recrystallization of the structure (see, for example, O'Neil and Taylor, 1967).

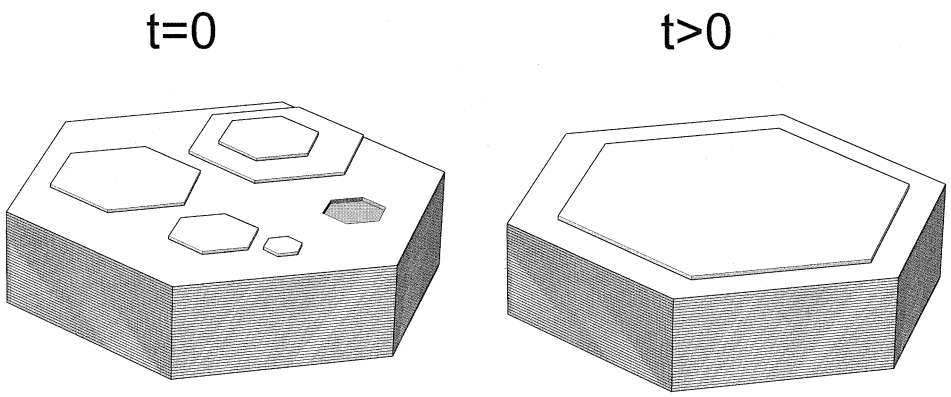

Fig. 7. Schematic illustration of the aging that we maintain controls the flux of ^{18}O from the surface of gibbsite, even where there is no detectable flux of protons or dissolved aluminum. The surface is constantly remaking itself by the motion of elementary steps on the surface. These motions create highly reactive monomers by hydrolyzing μ_2-OH bridges. The monomers release their ^{18}O to solution and this flux is detectable even though there is no net flux of mass from the mineral surface.

3) The μ_2-OH at the basal plane are *much* less reactive than in hydrolytic aqueous complexes, where rates of ligand exchange increase with the number of structural hydroxide ions. For example, Crimp et al. (1994) showed that ligand-exchange rates in aqueous Cr(III) complexes (monomers to tetramers) increase by up to $\sim 10^5$ as the OH/Cr ratio increases from 0 to 2. Our data on gibbsite indicate that this reactivity trend is reversed as more metals and hydroxide bridges are linked together into six-membered rings of μ_2-OH bridges in a solid like gibbsite. Therefore our measured rates of oxygen-isotope exchange are much slower than would be predicted by analogy with the aluminum polyoxocations (see Casey and Swaddle, 2003.)

Acknowledgments—This manuscript benefited greatly from the perceptive comments by Willem van Riemsdijk and two anonymous referees. Support for this research was from the U.S. NSF via grant EAR 0101246 and from the U.S. DOE DE-FG03-02ER15325. The authors also thank D. Winter and Profs. H. Spero and R. Zierenberg for help with the isotopic analyses and P. Green and Prof. T. Young for the ICP-MS analysis.

REFERENCES

Bloom P. R. (1983) The kinetics of gibbsite dissolution in nitric acid. *Soil. Sci. Soc. Am. J.* **47,** 164–168.

Bloom P. R. and Erich M. S. (1987) Effect of solution composition on the rate and mechanism of gibbsite dissolution in acid solutions. *Soil. Sci. Soc. Am. J.* **51,** 1131–1136.

Boudart M. (1976) Consistency between kinetics and thermodynamics. *J. Phys. Chem.* **80,** 2869–2870.

Casey W. H. and Swaddle T. W. (2003) Why small? The use of small inorganic clusters to understand mineral surface and dissolution reactions in geochemistry. *Rev. Geophys.* **41,** 1–20.

Casey W. H., Phillips B. L., Karlsson M., Nordin S., Nordin J. P., Sullivan D. J., and Neugebauer-Crawford S. (2000) Rates and mechanisms of oxygen exchanges between sites in the $AlO_4Al_{12}(OH)_{24}(H_2O)_{12}^{7+}$(aq) complex and water: Implications for mineral surface chemistry. *Geochim. Cosmochim. Acta* **64,** 2951–2964.

Casey W. H., Phillips B. L., and Furrer G. F. (2001) Aqueous aluminum polynuclear complexes and nanoclusters: a review. In *Nanoparticles in the Environment, Reviews in Mineralogy 44,* (eds. J. F. Banfield and A. N. Navrotsky) chap. 5, pp. 167–213. Mineral. Soc. America, Washington DC.

Charlet L. and Manceau A. A. (1992) X-ray absorption spectroscopic study of the sorption of Cr(III) at the oxide-water interface. *J. Coll. Interface Sci.* **148,** 443–458.

Cole D. R. and Chakraborty S. (2001) Rates and mechanisms of isotopic exchange. In *Stable Isotope Geochemistry* (eds. J. W. Valley and D. R. Cole) chap. 2. *Rev. Mineral. Geochem.* **43,** 82–191.

Crimp S. J., Spiccia L., Krouse H. R., and Swaddle T. W. (1994) Early stages of the hydrolysis of chromium(III) in aqueous solutions. 9. Kinetics of water exchange on the hydrolytic dimer. *Inorg. Chem.* **33,** 465–470.

d'Espinose de la Caillerie J. B., Kermarec M., and Clause O. (1995) Impregnation of γ-alumina with Ni(II) and Co(II) ions at neutral pH: hydrotalcite-type coprecipitate formation and characterization. *J. Am. Chem. Soc.* **117,** 11471–11481.

Furrer G. and Stumm W. (1986) The coordination chemistry of weathering: I. Dissolution kinetics of δ-Al_2O_3 and BeO. *Geochim. Cosmochim. Acta* **50,** 1847–1860.

Gastuche M. C. and Herbillon A. (1962) Étude des gels d'alumine: cristallisation en milieu désionisé. *Bull. Soc. Chim. Fr.* **1,** 1404–1412.

Hiemstra T., Yong H., and Van Riemsdijk W. H.. (1999) Interfacial charging behavior of aluminum (hydr)oxides. *Langmuir.* **15,** 5942–5955.

Mogollon J. L., Perez D. A., Lo Monaco S., Ganor J., and Lasaga A. C. (1994) The effect of pH, $HClO_4$, HNO_3 and ΔG_r on the dissolution rate of natural gibbsite using column experiments. *Mineral. Mag.* **58A,** 619–620.

Nagy K. L. (1995) Dissolution and precipitation kinetics of sheet silicates. In *Chemical Weathering Rates of Silicate Minerals* (eds. A. F. White and S. L. Brantley) chap. 5. *Rev. Mineral.* **31,** 173–225.

Nelmes R. J., Meyer G. M., and Tibballs G. E. (1982) The crystal structure of tetragonal KH_2PO_4 and KD_2PO_4 as a function of temperature. *J. Phys. Chem. Solid State Phys.* **15,** 59–75.

Nordin J. P., Sullivan D. J., Phillips B. L., and Casey W. H. (1998) An ^{17}O-NMR study of the exchange of water on $AlOH(H_2O)_5^{2+}$(aq). *Inorg. Chem.* **37,** 4760–4763.

O'Day P. A., Brown G. E., Jr., and Parks G. A. (1994) X-ray absorption spectroscopy of cobalt(II) multinuclear surface complexes and surface precipitates on kaolinite. *J. Coll. Interface Sci.* **165,** 269–289.

O'Neil J. R. and Taylor H. P. (1967) The oxygen isotope and cation exchange chemistry of feldspars. *Am. Mineral.* **52,** 1414–1437.

Peskleway C. D., Henderson G. S., and Wicks F. J. (2003) Dissolution of gibbsite: direct observations using fluid cell atomic force microscopy. *Am. Mineral.* **88,** 18–26.

Pulfer K., Schindler P. W., Westall J. C., and Grauer R. (1984) Kinetics and mechanisms of dissolution of bayerite (γ-$Al(OH)_3$) in HNO_3-HF solutions at 298.2 K. *J. Coll. Interface Sci.* **101,** 554–564.

Rosenqvist J., Persson P., and Sjöberg S. (2002) Protonation and charging of nanosized gibbsite (α-$Al(OH)_3$) particles in aqueous suspension. *Langmuir.* **18,** 4598–4604.

Saalfeld H. and Wedde M. (1974) Refinement of the crystal structure of gibbsite, $Al(OH)_3$. *Z. Kristallogr.* **139,** 129–135.

Scheidegger A. M., Strawn D. G., Lamble G. M., and Sparks D. L. (1998) The kinetics of mixed Ni-Al hydroxide formation on clay and aluminum oxide minerals: A time-resolved XAFS study. *Geochim. Cosmochim. Acta* **13,** 2233–2245.

Strandh H (1999) Mineral dissolution from molecular to field scale. Ph. D. thesis, University of Stockholm, 102 pp.

Temkin M. I. (1971) The kinetics of steady-state complex reaction. *Internat. Chem. Eng.* **11,** 709–717.

Thompson H. A., Parks G. A., and Brown G. E., Jr.. (1999) Dynamic interactions of dissolution, surface adsorption, and precipitation in an aging cobalt(II)-clay-water system. *Geochim. Cosmochim. Acta* **63,** 1767–1779.

Walter T. H. and Oldfield E. (1989) Magic angle spinning oxygen-17 NMR of aluminum oxides and hydroxides. *J. Phys. Chem.* **93,** 6744–6751.

Wesolowski D. J. and Palmer D. A. (1994) Aluminum speciation and equilibria in aqueous solutions: V. Gibbsite solubility at 50°C and pH 3–9 in 0.1 molal NaCl solutions (a general model for aluminum speciation; analytical methods). *Geochim. Cosmochim. Acta* **58,** 2947–2969.

APPENDIX I

Converting $\delta^{18}O$ Values to the Molarity Scale

Unlike most studies of oxygen-isotope exchange in minerals, we need to calculate the concentration in molar units, not in per mil values relative to an accepted standard, such as SMOW. To establish the molar concentrations, we constructed a standard curve [Figure A1] from highly enriched stock solutions of $H_2{}^{18}O$ and used this standard curve to convert the measured $\delta^{18}O$ values into molar units. Solutions with different contents of $H_2{}^{18}O$ were prepared by diluting weighted amounts of a 7.4% $H_2{}^{18}O$ stock solution (Isotec Labs). Because the fluxes of ^{18}O into the solution are unaffected by constant, systematic offset in ^{18}O concentration, we defined the concentration of $H_2{}^{18}O$ in the 18 MΩ cm^{-1} water that we used for the standards, and in all the experiments, as a baseline. The concentration of ^{18}O in standards and samples were then expressed as *excess* ^{18}O over this baseline and the time-rate of change of ^{18}O concentrations yielded the flux.

Figure A1 shows the calculated concentrations of $H_2{}^{18}O$ in the standards versus the measured $\delta^{18}O$ values. A least-squares optimization was performed to obtain the mathematical relationship between the $\delta^{18}O$ values (in per mil) and the concentration of ^{18}O (in mM). The precision and accuracy of the obtained values were checked by repeated analysis of samples and standards. Small uncertainties in the standard curve, or the calculation of molar ^{18}O concentration, do not affect the essential results.

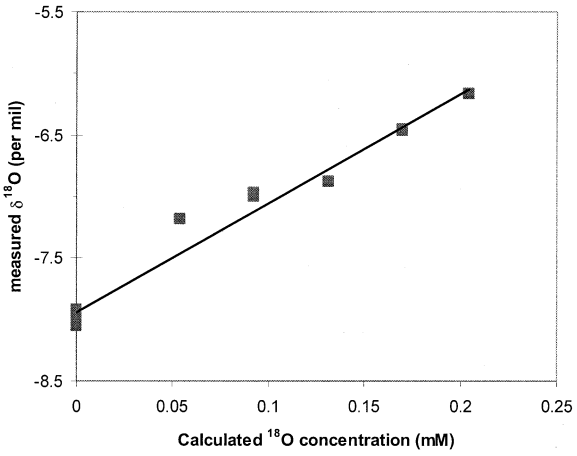

Fig. A1. Calibration curve for converting measured $\delta^{18}O$ values into molar units.

Calculating the Depth of ^{18}O Enrichment into the Mineral

The average density of μ_2-OH sites was calculated by assuming that one third of the total surface area was at the particle edges, as is indicated in the electron micrographs [Figure 1]. This assumption results in an average density (ρ_{OH}) of 24.4 μ_2-OH sites per nm^2 per gibbsite layer. To calculate the density of ^{18}O in the surface layers of the gibbsite particles, ρ_{OH} value was multiplied by the mole fraction of ^{18}O (C_{tag}) in the tagging solution:

$$\rho_{OH} * 10^{18}\ nm^2/m^2 * C_{tag}/N_A = {}^{18}O\text{-moles}/m^2 \text{ on gibbsite basal surface} \quad (A1)$$

The total amount of ^{18}O contained in the particle is measured by completely digesting the solid in acid and measuring the resulting concentration of ^{18}O in the solution. The total amount of ^{18}O contained in the gibbsite particles can be calculated from this measured ^{18}O concentration (C_{meas}) of the solution, the specific surface area (SA) of the solid and the solid concentration of the suspension (S):

$$C_{meas}/(SA * S) = {}^{18}O\text{-moles}/m^2 \quad (A2)$$

Dividing the value given by Eqn. (A2) by the value from Eqn. (A1) yields the number of surface layers that were enriched in ^{18}O to give the measured concentration of ^{18}O in the solution after complete digestion in acid.